Geogr. Fis. Dinam. Quat.
39 (2016). 89-100, 10 figg., 1 tabb.

DOI 10.4461/GFDQ. 2016.39.9

ANTONELLA SENESE (*), MAURIZIO MAUGERI (**), STEFANO FERRARI (***),
GABRIELE CONFORTOLA (***), ANDREA SONCINI (***),
DANIELE BOCCHIOLA (***) & GUGLIELMINA DIOLAIUTI (*)

MODELLING SHORTWAVE AND LONGWAVE DOWNWARD RADIATION AND AIR TEMPERATURE DRIVING ABLATION AT THE FORNI GLACIER (STELVIO NATIONAL PARK, ITALY)

ABSTRACT: A. SENESE, M. MAUGERI, S. FERRARI, G. CONFORTOLA, A. SONCINI, D. BOCCHIOLA & G.A. DIOLAIUTI. *Modelling shortwave and longwave downward radiation and air temperature driving ablation at the Forni Glacier (Stelvio National Park, Italy).* (IT ISSN 0391-9838, 2016)

We focus here on modelling the meteorological parameters most influencing snow/ice melting over an alpine glacier. Specifically, we consider shortwave and longwave downward radiation, and air temperature. We set up and test a methodology for their accurate distribution at the glacier surface, which can be applied whenever: i) supraglacial meteorological measurements are available or ii) weather data are acquired from a station quite close to the glacier. As a suitable site to test our approach we selected the Forni Glacier, in the Italian Alps, where an Automatic Weather Station (AWS) has been running since autumn 2005 thus giving a robust dataset for developing a field based modeling approach. First, we modelled and distributed the incoming solar radiation by taking into account actual atmospheric conditions, glacier topography and shading. Then, we modelled the incoming longwave radiation considering cloud-cover and air temperature. Third, we investigated a local lapse rate to depict the yearly variability of the vertical air temperature gradient, to assess the actual thermal conditions at different elevations. Finally, we compared the modeled values against data collected on the field. The results display that during the glacier ablation period (i.e.: May-September): i) our approach provides a good depiction of both point incoming solar and infrared radiation fluxes, ii) the spatial distribution of the incoming solar radiation we developed is satisfactory, iii) our tests suggest that the incoming longwave fluxes can be considered constant over the whole glacier ablation area thus neglecting its spatial distribution, and iv) the application of a local lapse rate provides a good distribution of air temperature at the glacier surface.

KEY WORDS: Short- And Long-Wave Downward Radiation; Air Temperature; Ice And Snow Melting; Alpine Glaciers, Stelvio National Park

(*) *Dipartimento di Scienze della Terra, Università degli Studi di Milano, Italy.*

(**) *Dipartimento di Fisica, Università degli Studi di Milano, Italy.*

(***) *Dipartimento di Ingegneria Civile e Ambientale, Politecnico di Milano, Italy.*

Corresponding author: antonella.senese@unimi.it

The AWS1 Forni is part of the SHARE (Stations at High Altitude for Research on the Environment) network; SHARE is an international program developed and managed by the Ev-K2-CNR Association. It was also included in the former CEOP network (Coordinated Energy and Water Cycle Observation Project), promoted by the WCRP (World Climate Research Programme) within the framework of the online GEWEX project (Global Energy and Water Cycle Experiment), and in the SPICE (Solid Precipitation Intercomparison Experiment) project managed and promoted by the WMO (World Meteorological Organization). The long sequence of meteorological and glaciological data also permitted the insertion of the AWS1 Forni into CryoNet project (core network of Global Cryosphere Watch promoted by the WMO). This research was achieved under the umbrella of the SHARE-Stelvio project, funded by the Lombardy Region government, lead by G Diolaiuti (PI) and managed by FLA (Lombardy Foundation for the Environment) and Ev-K2-CNR Association. This study was also funded by DARAS (Department of regional affairs, autonomies and sport) of the Presidency of the Council of Ministers of the Italian government through the GlacioVAR project. Moreover, Sanpellegrino Spa brand Levissima kindly supported data analyses. The authors wish to thank the Lombardy Regional Agency for Environmental Protection (ARPA Lombardia) and the "a2a energia spa" company (an Italian energy supplier) who kindly provided meteorological data useful for our modelling approach.

RIASSUNTO: A. SENESE, M. MAUGERI, S. FERRARI, G. CONFORTOLA, A. SONCINI, D. BOCCHIOLA & G.A. DIOLAIUTI. *Modellazione della radiazione entrante (ad onda corta e lunga) e della temperatura dell'aria responsabili della fusione glaciale. Caso studio: il Ghiacciaio dei Forni (Parco Nazionale dello Stelvio, Italia).* (IT ISSN 0391-9838, 2016)

Nel presente lavoro viene proposta una metodologia per la modellazione dei parametri meteorologici maggiormente influenti sulla fusione di neve e ghiaccio di un ghiacciaio alpino: la radiazione entrante sia ad onda lunga (atmosferica) che ad onda corta (solare) e la temperatura dell'aria. Per la distribuzione di questi parametri è stato sviluppato un approccio da applicare qualora siano disponibili: i) misure dei parametri meteorologici rilevati sulla superficie del ghiacciaio (che consentano l'acquisizione diretta delle informazioni energetiche e meteorologiche) o ii) dati meteorologici acquisiti nelle immediate vicinanze di esso. Per la verifica del metodo proposto abbiamo scelto il più grande ghiacciaio vallivo italiano, il Ghiacciaio dei Forni, nel Parco Nazionale dello Stelvio, dove dal 2005 è in funzione una stazione meteorologica automatica (AWS), le cui acquisizioni hanno permesso di popolare un lungo e praticamente ininterrotto data-base utile alla validazione. La prima fase della ricerca ha visto la distribuzione della radiazione solare entrante in funzione delle condizioni atmosferiche reali, della topografia glaciale e dell'ombreggiamento. La seconda fase ha riguardato la modellazione della radiazione ad onda lunga

entrante sulla base della copertura nuvolosa e della temperatura dell'aria. Infine abbiamo ricercato un gradiente termico verticale locale per riprodurre la variabilità annuale della temperatura in quota e per descrivere le condizioni termiche alle diverse altitudini. Una volta parametrizzati tutti i fattori abbiamo confrontato quanto ottenuto con i dati meteorologici ed energetici acquisiti alla superficie del Ghiacciaio dei Forni dalla stazione meteo permanente. Il confronto, condotto per i mesi durante i quali avviene fusione sul ghiacciaio e per i quali è dunque importante disporre di dati utili alla sua modellazione e quantificazione (Maggio-Settembre) ha evidenziato che: i) il nostro approccio permette di predire con accuratezza a livello puntuale i flussi radiativi in entrata sia ad onda corta che ad onda lunga; ii) la distribuzione spaziale della radiazione ad onda corta da noi modellata è soddisfacente; iii) i nostri test suggeriscono che la radiazione ad onda lunga entrante si possa considerare spazialmente costante su una stessa area glaciale alpina permettendo pertanto di trascurare la sua distribuzione spaziale e limitandosi alla modellazione temporale puntuale e iv) l'applicazione di un gradiente termico verticale permette di meglio distribuire la temperatura dell'aria alle diverse fasce altitudinali glaciali.

TERMINI CHIAVE: Radiazione Entrante Ad Onda Corta E Ad Onda Lunga; Temperatura Dell'aria; Fusione Della Neve E Del Ghiaccio; Ghiacciai Alpini, Parco Nazionale dello Stelvio

1. INTRODUCTION AND AIMS

A large variety of snow and ice melt models was developed hitherto, ranging from physically based energy-balance models (e.g. Brun & *alii*, 1989; Bloschl & *alii*, 1991; Arnold & *alii*, 1996; Bocchiola & *alii*, 2015), to empirical methods driven by one or more meteorological variables, mainly by air temperature (e.g. Braithwaite, 1995). Radiation fluxes generally prevail in the glacier energy balance, and shortwave radiation is often the dominant incoming flux (Senese & *alii*, 2012a). However, incoming longwave radiation can contribute similar or higher amounts of energy during cloudy periods because of increased atmospheric emissivity (e.g. Müller, 1985; Granger & Gray, 1990). When the albedo of snow is high, surface net radiation and melt energy can be higher under overcast skies than under clear skies (e.g. Bintanja & Van den Broeke, 1996). Although melt rates are fully described through the surface energy budget, glacier melt models based upon computation of the energy fluxes are not always applicable in mountain and remote areas, and in particular at the surface of glaciers, due to lack of input data. In fact, in high-mountain glacierized regions automatic weather stations (AWSs) measuring radiation fluxes are available in few locations, and more often placed outside glaciers. AWSs are generally equipped in order to provide useful radiative data to describe glacier surface conditions, in particular the solar fluxes and the albedo. Unfortunately, several AWSs are not equipped with sensors measuring longwave radiation as well.

Accordingly, some approaches have to be developed to model radiative inputs (both short- and long-wave ones) at the surface of mountain glaciers in order to compute their energy budget and then to evaluate the melting rates and amount. Concerning incoming solar flux, the approach proposed by Iqbal (1983) improved accuracy over more conventional approaches as reviewed by Gueymard (1993), since it allows to obtain the irradiance components with an accuracy comparable to routine measurements. Concerning incoming longwave radiation, a review of models is given by Ellingston & *alii* (1991). Longwave radiation is usually estimated from empirical relationships against air temperature and vapour pressure (Plüss & Ohmura, 1997; Oerlemans, 2000; Klok & Oerlemans, 2002; Hock, 2005), based on standard meteorological measurements (Kondratyev, 1969).

In this context, this paper aims at developing and testing a simple and replicable methodology for modelling input radiative (both short- and long-wave) fluxes and air temperature and for distributing them over the whole ablation surface of a mountain glacier. In particular, our approach is thought to be applied starting from meteorological data which have not necessary to be acquired with an AWS at the glacier surface but have just to be sampled quite close to the glacier surface.

A suitable site to test our approach is the Forni Glacier (Stelvio National Park, Italian Alps), the largest Italian valley glacier (11.36 km^2 in area, D'Agata & *alii*, 2014), where since September 2005 an automatic weather station (AWS1 Forni) has been continuously running (Citterio & *alii*, 2007; Senese & *alii*, 2012a; 2012b; 2014; Gambelli & *alii*, 2014; Azzoni & *alii*, 2016; Fugazza & *alii*, 2016), thus assuring a long sequence of supraglacial meteorological and energy data.

2. METHODS

2.1. *Temperature and radiative measurements: the AWS1 Forni and the portable station*

Since autumn 2005 a meteorological and energy dataset recorded by an automatic weather station on the ablation tongue of the Forni Glacier (AWS1 Forni, WGS84 coordinates 46°23'56.0" N and 10°35'25.2" E, at 2631 m a.s.l., fig. 1) provides information of the micrometeorological conditions and the energy fluxes driving snow/ice ablation. This dataset is mostly uninterrupted (since 26/09/2005 up to now), with very few gaps (3.05% of the total period, Senese & *alii*, 2014). The AWS1 Forni is powered by two solar panels (40 Watt) and a lead-gel battery (100 Ah). Data points are sampled at 60-second intervals and averaged over a 30-minute time period for most of the sensors (see Senese & *alii*, 2012a), including the basic distribution parameters (minimum, mean, maximum, and standard deviation values).

During summer 2011 and 2012 (30 June 2011, 4 July and 9 September 2012), field surveys were carried out at the Forni Glacier tongue, to collect a total sample of 18 radiation measurements (Azzoni & *alii*, 2016). The portable station was equipped with a four component radiometer (CNR1, Kipp&Zonen, with an accuracy of ±5%), a waterproof box containing a data logger (E-log, LSI-Lastem), a 5 Ah battery, a 10W solar panel and a tripod to raise the net radiometer above the ice surface (fig. 2) for short periods (c. 20-30 min for each measurement). The CNR1 net radiometer used here is of the same type as that running at the AWS1 Forni (Citterio & *alii*, 2007; Senese & *alii*, 2012a), therefore providing homogeneity of the two datasets. Data acquisition rate is every second, and then every 5 minutes (during 2011) and every minute (during 2012), minimum, average, maximum and standard deviation values were calculated and recorded.

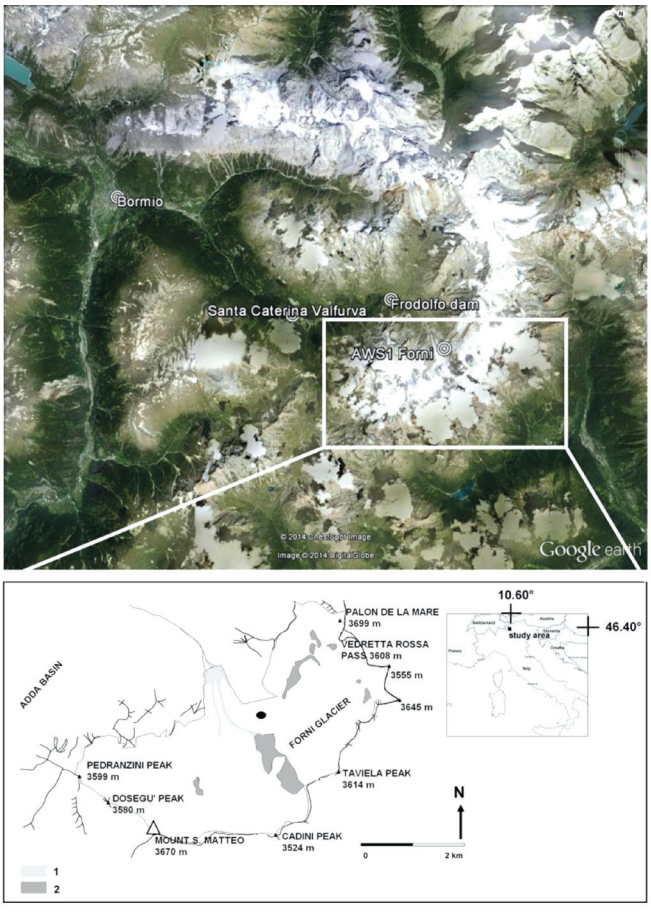

FIG. 1 - The location of Bormio, S. Caterina Valfurva, Frodolfo dam and the Forni Glacier (Google Earth © raster base) and in the lower picture the location of the AWS1 Forni (black dot). In this latter map the light grey areas (1) are used to mark supraglacial debris coverage and the dark grey zones (2) indicate rock exposures and nunataks.

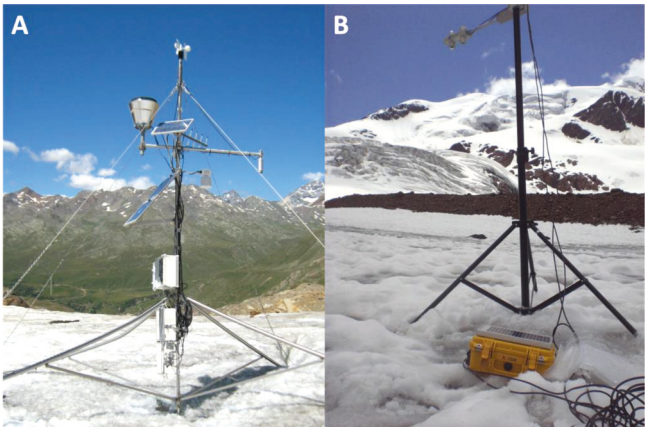

FIG. 2 - The two supraglacial automatic weather stations: on the left the permanent AWS1 Forni (A), and on the right the portable net radiometer (B).

2.2. *Incoming solar radiation model*

To model the distributed incoming solar radiation at the Forni Glacier surface, we used four methods of increasing complexity, namely considering i) a flat and ideal exo-atmospheric surface (i.e. we calculated radiation taking into account astronomical and geographical factors only, thus neglecting atmospheric absorption and orography, Iqbal, 1983; Allen & *alii*, 2006; Wang & *alii*, 2006), ii) a sloped exo-atmospheric surface (i.e. we considered slope and aspect too, Garner & Ohmura, 1968; Duffie & Beckman, 1980; Hunter & Goodchild, 1997; Allen & *alii*, 2006), iii) a sloped exo-atmospheric surface in a complex orographic system (i.e. we evaluated the shading too), and iv) a complex surface (from iii) in an actual atmosphere (i.e. we also considered meteorological conditions, and the multireflection from the surrounding surfaces, Hock & Noetzli, 1997; Gueymard, 2001). We describe here the algorithms we applied to distribute the global radiation.

i) The approach proposed by Iqbal (1983) was used to estimate the daily exo-atmospheric solar radiation ($SW_{0\text{-}point}$) received by a flat surface:

$$SW_{0-point} = I_0 \cdot E_0 \cdot k \cdot \int_{w_{sr}}^{w_{ss}} \cos(\theta) \cdot dh \qquad (1)$$

where I_0 is average solar irradiance at the mean Earth-Sun distance (1367 W m^{-2}), E_0 is an eccentricity factor (i.e. the correction due to the elliptical orbit of the Earth depending on the day of the year; Spencer, 1971), θ is the angle between the normal to the surface and the solar beam (Oke, 1987), h is the hour angle (zero value at solar noon, negative during morning and positive during afternoon), and k is a factor to express $SW_{0\text{-}point}$ in MJ day^{-1}. Finally, w_{sr} and w_{ss} are the sunrise and sunset hour angles, respectively (Allen & *alii*, 2006):

$$w_{ss} = arccos(-\tan \Phi \cdot \tan \delta) \qquad (2)$$

$$w_{sr} = -w_{ss} = -arccos(-\tan \Phi \cdot \tan \delta) \qquad (3)$$

where Φ is the latitude, and δ is the solar declination. Here, w_{sr} and w_{ss} have opposite values because the hour angle is the angular displacement of the sun, east or west of the local meridian. This is due to rotation of the Earth on its axis, at 2π/24 radiant per hour: morning (w_{sr}) is assumed as negative and afternoon (w_{ss}) as positive. Finally, simplifying the approach proposed by Wang & *alii* (2006), the daily exo-atmospheric solar radiation received by a flat surface is:

$$SW_{0-point} = 2 \cdot I_0 \cdot E_0 \cdot k \cdot [(\sin \delta \cdot \sin \Phi) \cdot w_{ss} + (\cos \delta \cdot \cos \Phi) \cdot \sin w_{ss}] \qquad (4)$$

ii) For an inclined surface, we considered the angle between the normal to the surface and the solar beam, by expressing Eqn 4 according to Garner & Ohmura (1968) and Duffie & Beckman (1980) as:

$$SW_{0-point} = I_0 \cdot E_0 \cdot k \cdot [(\sin\delta \cdot \sin\Phi \cdot \cos S) \cdot (w_{ss} - w_{sr}) - (\sin\delta \cdot \cos\Phi \cdot \cos S \cdot \cos A) \cdot (w_{ss} - w_{sr}) + (\cos\delta \cdot \cos\Phi \cdot \cos S) \cdot (\sin w_{ss} - \sin w_{sr}) + (\cos\delta \cdot \sin\Phi \cdot \sin S \cdot \cos A) \cdot (\sin w_{ss} - \sin w_{sr}) - (\cos\delta \cdot \sin A \cdot \sin S) \cdot (\cos w_{ss} - \cos w_{sr})] \quad (5)$$

where S is the slope angle and A is the aspect angle, both calculated according to Hunter & Goodchild (1997). The slope ranges from 0° (i.e. horizontal) to 90° (i.e. vertical). The aspect is related to the South, then 0° represents South, 90° East, -90° West, and ±180° North. To calculate w_{sr} and w_{ss} for an inclined surface we applied the method proposed by Allen & *alii* (2006). Also the auto-shading was estimated following the approach reported by Allen & *alii* (2006): when slopes are steep and northerly facing in northern latitudes or southerly facing in southern latitudes, the grid point may be shaded during all or portions of the day.

iii) To assess whether a grid point is affected by shading (i.e. the orography intercepts the hypothetical line linking this grid point to the Sun), we considered both Sun elevation angle (γ_{Sun}), and the angle between the mountain peak and the grid point ($\gamma_{peak\text{-}point}$):

$$\gamma_{Sun} = arcsin[cos(\omega) \cdot cos(\delta) \cdot cos(\phi) + sin(\phi) \cdot sin(\delta)] \quad (6)$$

and

$$\gamma_{peak-point} = \arctan\left(\frac{h_{peak} - h_{point}}{distance\ peak-point}\right) \quad (7)$$

where h_{peak} and h_{point} are the mountain peak and grid point elevations, respectively, defined by the DEM (i.e. Digital Elevation Model). In particular, we searched for the $\gamma_{peak\text{-}point}$ value representing the highest obstructing angle along the grid-point-to-the-Sun direction for each hour of the day. In fact, almost every glacier point featured different values of h_{peak}, and these also varied with the solar azimuth. Hence, whenever $\gamma_{Sun} < \gamma_{peak\text{-}point}$ the grid point is affected by shading.

iv) To take into account the atmospheric absorption, we considered the ratio between the global radiation actually received by a surface measured by the AWS1 Forni ($SW_{T\text{-}AWS}$), and the modelled exo-atmospheric radiation received by the same surface ($SW_{0\text{-}AWS}$) (Gueymard, 2001):

$$SW_T = \frac{SW_{T-AWS}}{SW_{0-AWS}} \cdot SW_0 \quad (8)$$

The $SW_{T\text{-}AWS}/SW_{0\text{-}AWS}$ ratio will vary from a maximum under clear-sky conditions to a minimum in overcast conditions. This ratio was calculated at the AWS1 Forni site, and the value was considered representative for the whole glacier surface (Escher-Vetter, 1980). The incoming solar radiation ($SW_{T\text{-}AWS}$) was measured at the radiometer installed at the AWS1 Forni, whereas the exo-atmospheric radiation ($SW_{0\text{-}AWS}$) was estimated according to Eqn 5, taking into account the slope of the surface where the meteorological station is located.

The AWS1 Forni is located on a valley glacier, and therefore it is potentially subject to topographic shading, while other parts of the glacier may still be in the sunshine. For this reason, five cases (i.e.: A-B-C-D-E here following) were distinguished for the calculation of the incoming solar radiation at any grid point of the glacier ($SW_{T\text{-}point}$), depending on whether or not the AWS and the grid point featured shading due to surrounding topography according to Eqns 6-7 (Hock & Noetzl, 1997):

A) Both AWS and grid point are unshaded at the time t:

$$SW_{T-point}(t) = \frac{SW_{T-AWS}(t)}{SW_{0-AWS}(t)} \cdot SW_{0-point}(t) \quad (9)$$

B) Grid point is in the sun and AWS in the shade at the time t:

$$SW_{T-point}(t) = \left(\frac{SW_{T-AWS}(t^*)}{SW_{0-AWS}(t^*)}\right) \cdot SW_{0-point}(t) \quad (10)$$

where t^* is the time closest to t with the station in sunny conditions (i.e. not shaded). As the AWS site is more shaded in the morning than in afternoon, t^* occurs generally later than t with an average lag of about 30 minutes. Cloud conditions are assumed to remain constant during this period of time. However, the error introduced by this assumption is considered small as topographic shading of the AWS will only occur during times of low sun altitude, when global radiation tends to be small (Hock & Holmgren, 2005).

C) Both AWS and grid point are shaded at the time t:

$$SW_{T-point}(t) = SW_{T-AWS}(t) \quad (11)$$

There is no direct radiation, but only diffuse radiation at both grid points. Diffuse radiation is assumed to be invariant over the area. Hence, global radiation at the grid point is set to measured global radiation.

D) Grid point is shaded and AWS is unshaded, in clear-sky and partially cloudy conditions at the time t:

$$SW_{T-point}(t) = 0.15 \cdot SW_{T-AWS}(t) \quad (12)$$

There is both direct and diffuse radiation at the AWS but only diffuse radiation at the grid point. This latter is approximated using a fixed percentage of 15%. Indeed, following Konzelmann & Ohmura (1995), the diffuse radiation is ~15% of the total amount of incoming solar radiation.

E) Grid point is shaded and AWS is unshaded, under overcast conditions at the time t:

$$SW_{T-point}(t) = SW_{T-AWS}(t) \quad (13)$$

where the diffuse radiation is 100% of the total radiation and the shading is irrelevant.

To evaluate the accuracy of the modelled solar data ($SW_{T\text{-}point}$), we compared the calculated values against shortwave radiation data measured on the field by the portable radiometer during summer 2011 and 2012 (18 sites). In high-mountain regions the temporal variability of cloudiness is very high, and it influences the $SW_{T\text{-}AWS}/SW_{0\text{-}AWS}$ ratio whenever this latter is evaluated with a high time resolution (e.g. every 5 minutes or higher). This phenomenon could affect partially our computations, since we derived the $SW_{T\text{-}AWS}/SW_{0\text{-}AWS}$ ratio from AWS1 Forni data (which recorded at thirty minutes interval), while our portable radiometer acquired data every 5 minutes in 2011, and every minute in 2012. In order to minimize such discrepancy we calculated the ratio considering the half-hourly minimum, mean and maximum solar values acquired by the AWS1 Forni.

2.3. *Incoming infrared radiation model*

In the available literature concerning the estimation of distributed ice melt using an energy budget, both the incoming and the outgoing infrared radiation are often taken constant in space (e.g. Hock & Noetzli, 1997). However, incoming longwave radiation depends on air temperature and humidity (varying over the glacier surface as well), on topographic reflection, and on spatial cloud-cover variations.

To investigate the suitability of a spatially constant value to describe at each time step the infrared radiation over the whole ablation surface of a glacier, we performed field measurements of incoming longwave radiation (i.e. LW_{in}) at different sites spread over the Forni Glacier tongue. The surveys were carried out with the portable radiometer (CNR1) during the ablation season in 2011 and 2012. We then compared these field measurements with the values recorded by the AWS1 Forni. In figure 3 two examples are shown: one in summertime 2011 (series with circles) and one in summertime 2012 (series with diamonds). As expected, the spatially distributed longwave measurements (black series, fig. 3) resulted in the range measured by the AWS1 Forni (white series, fig. 3). Hence, the assumption of spatially constant incoming longwave radiation may be taken as acceptable (as stated by Hock & Noetzli, 1997).

We also considered that mostly supraglacial AWSs are not equipped with a four component radiometer (i.e. a net radiometer measuring both up- and down-ward, and short- and long-wave fluxes) but only with a global solar sensor, thus limiting the evaluation of the radiation to the shortwave contribution, and neglecting the longwave one. We therefore sought for a method to model incoming longwave radiation, applicable also in sites where a longwave radiometer is not available. The solution we found the most suitable uses air temperature (T_a) and sky emissivity (ε) as main input data. In fact, in melt models, longwave irradiance is usually estimated from empirical relationships, based on

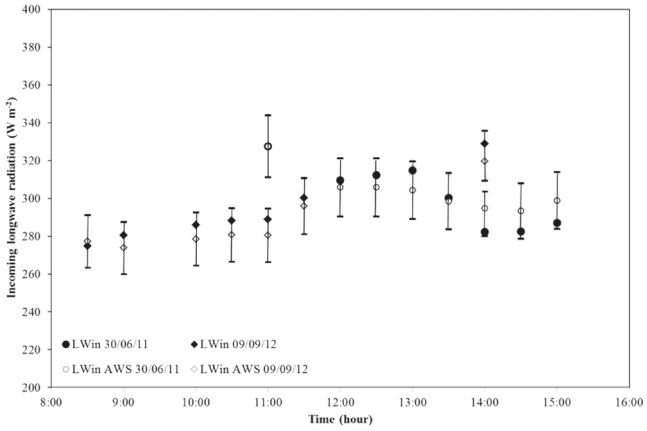

FIG. 3 - Comparison of LW_{in} data acquired at several glacier sites (black series) with LW_{in} values recorded in the same time frames by the AWS1 Forni (white series). The circles refer to measurements acquired on 30th of June 2011, and the diamonds on 9th of September 2012. On X axis time (hours) is reported, on Y axis LW_{in} values are indicated (W m^{-2}). The vertical bars show an error range of ± 5% of the measured value (error reported by Kipp&Zonen).

standard meteorological measurements, exploiting the fact that longwave irradiance correlates well with air temperature and vapour pressure at screen level, usually at 2 m above the surface (Kondratyev, 1969).

The sky emissivity was calculated from cloudiness (n, assessed from incoming solar radiation from the AWS1 Forni) and vapour pressure (e_a, estimated from air temperature and relative humidity values from the AWS1 Forni). Hence, in order to model LW_{in}, a thermo-hygrometer and a global radiometer (both commonly-used sensors) are necessary. In fact, the incoming infrared component firstly depends upon cloudiness. As cloud observations are not available at the Forni Glacier (nor at other sides nearby), cloudiness was estimated from the measured incoming shortwave radiation dataset ($SW_{T\text{-}AWS}$) (Oerlemans, 2000). First, the daily global radiation (W m^{-2}) for clear sky was estimated ($SW_{T\text{-}CS}$) by way of a sine-cosine function (fig. 4), adjusted on the daily measured data averaged from

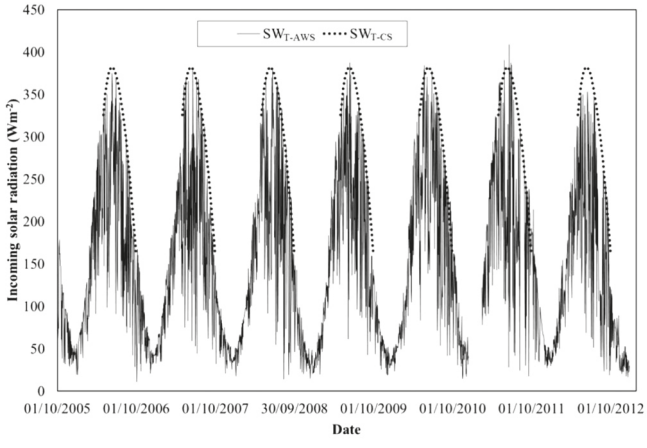

FIG. 4 - Clear sky envelope ($SW_{T\text{-}CS}$) defined for incoming solar radiation (truncated Fourier series at the second factor) and the actual daily mean values ($SW_{T\text{-}AWS}$) from 1st October 2005 to 31st December 2012.

2006 to 2012 and interpolated through the truncated Fourier series at the second order below:

$$SW_{T-CS} = 160.4 - 236.0 \cdot \cos\left(\frac{day \cdot 2\pi}{365}\right) + 27.3 \cdot \quad (14)$$

$$\cdot \sin\left(\frac{day \cdot 2\pi}{365}\right) - 25.1 \cdot \cos\left(2\frac{day \cdot 2\pi}{3{,}65}\right) - 15.1 \cdot \sin\left(2\frac{day \cdot 2\pi}{365}\right)$$

where *day* is the Julian date. To assess the actual clear sky incoming solar radiation without overestimation as due to multiple reflection from snow covered surroundings, we considered the snow-free half-year (i.e. from 1 May to 30 September of every year, following Oerlemans, 2000). Year 2005 was excluded by this computation because the AWS1 Forni dataset starts from 26th September 2005.

Then, the atmospheric transmissivity (τ) depending on the cloud cover is defined by:

$$\tau = \frac{SW_{T-AWS}}{SW_{T-CS}} \quad (15)$$

and then the cloudiness (n), based on the altitude, was estimated according to the approach proposed by Sauberer (1955) and Konzelmann & *alii* (1994):

$$\tau = 1 - (0.41 - 6.5 \cdot 10^{-5} \cdot altitude)\, n - 0.37\, n^2 \quad (16)$$

with an altitude of the AWS1 Forni site of 2631 m a.s.l. (fig. 5). This relation was found analysing global radiation data from Austrian climate stations (Alps), thus it can be assumed representative for the Forni Glacier. On days when τ exceeds 1, cloudiness is zero.

Once we estimated cloudiness, we took into account the effect of emissivity for clear (ε_{cs}) and overcast (ε_{cl}) sky. The latter can be considered constant and close to one (0.976 at 2310 m a.s.l., Greuell & *alii*, 1997), since clouds block longwave radiation very effectively (Oerlemans, 2000). Otherwise, the clear-sky emissivity depends on the (lumped) concentration of greenhouse gases, and on vapour pressure (e_a) and air temperature (T_a) according to Konzelmann & *alii* (1994):

$$\varepsilon_{cs} = 0.23 + b\left(\frac{e_a}{T_a}\right)^{1/8} \quad (17)$$

with $b = 0.475$ (found by Oerlemans, 2001, at 2310 m a.s.l.). The values of e_a and T_a were those recorded by the AWS1 Forni. Then the total emissivity is:

$$\varepsilon = \varepsilon_{cs}(1 - n^p) + \varepsilon_{cl} n^p \quad (18)$$

with $p = 2$. Cloud emission is often calculated from observations of cloud cover, type and altitude. However, this information is rarely available in remote locations and it is subject to errors. Sicart & *alii* (2006) in the mountains of northern Canada, and Sedlar & Hock (2009) on a glacier in northern Sweden, showed that a rough estimate of atmospheric solar transmissivity from measurements of global radiation can be used as an acceptable index of cloud cover to parameterize cloud emissivity.

Finally, the incoming longwave radiation was assessed following the Stephan-Boltzmann law:

$$LW_{in} = \varepsilon \cdot \sigma \cdot {T_a}^4 \quad (19)$$

where σ is 5.67 x 10^{-8} W m^{-2} K^{-4}. The method was verified by comparison of the modelled data against the 7-year infrared flux dataset recorded by the AWS1 Forni (from 1st October 2005 to 31st December 2012).

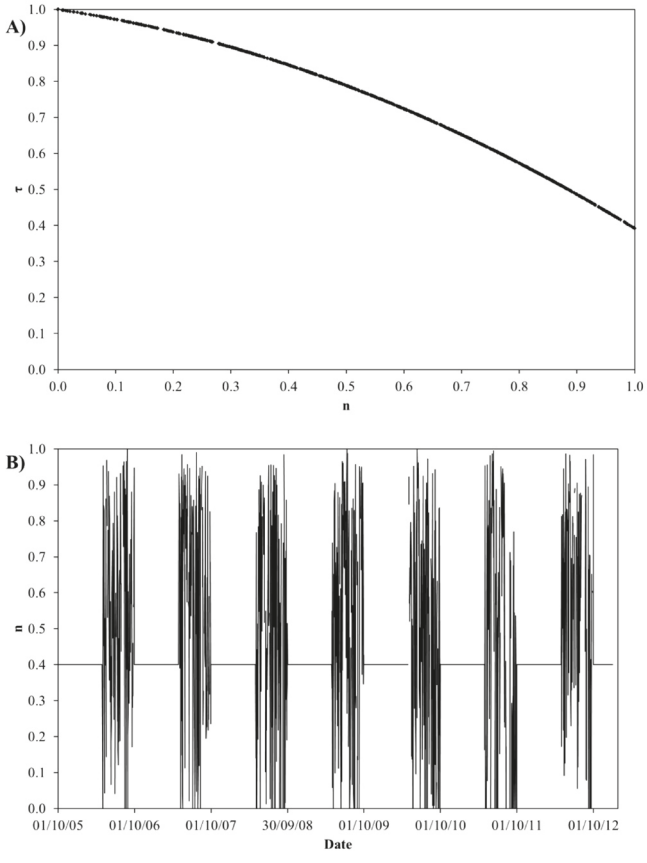

FIG. 5 - A) The relation between the daily cloudiness (n) and the atmospheric transmissivity (τ), and B) the daily cloudiness (n) from 2005 to 2012.

2.4. Air temperature model

To assess the most suitable lapse rates applicable also in other periods, we considered i) long temperature records, ii) different measurement stations, and iii) general meteorological conditions (such as excluding thermal inversion). We processed 4 years of data (from 1st January 2006 to 31st December 2009) from Bormio (1225 m a.s.l.), Santa Caterina Valfurva (1730 m a.s.l.) and Frodolfo dam (2180 m a.s.l.) weather stations (nearby the Forni Glacier, fig. 1). We firstly calculated hourly series of lapse rates between the three surrounding weather stations and the AWS1 Forni, thus obtaining for each year 3 dataset of hourly data records, thus 12 sets of hourly lapse rate. Secondly to avoid thermal inversion to affect the data too much, only the warmest hours of the day (from 12 pm to 4 pm) were considered in the calculation of the daily average lapse rates.

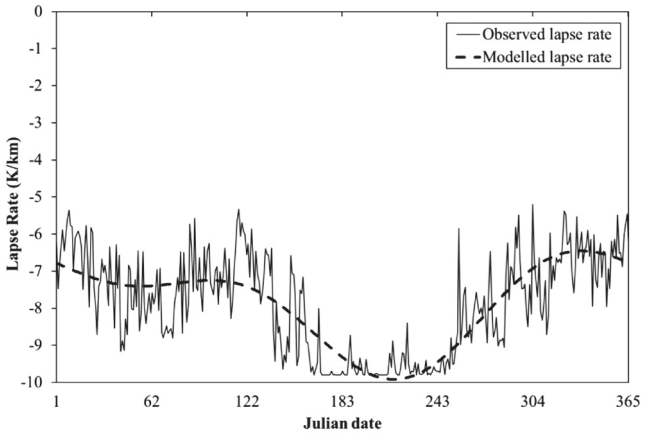

FIG. 6 - Daily averaged lapse rate considering only the hottest hours per day (from 12 am to 4 pm, "observed" in the legend) and the smoothed daily values obtained by a truncated Fourier series at the second order ("modelled" in the legend).

Indeed in a previous study (Senese & *alii*, 2014) Santa Caterina Valfurva and the Frodolfo dam AWSs were found to be affected by thermal inversion for about 9% and 1% from 2006 to 2012, respectively. Thirdly, these 12 series of daily records were averaged, to obtain annual daily lapse rate. Finally, to smooth this record, a regression model was used (fig. 6). More precisely, we used a relationship between lapse rate (λ) and time (*day*), following a truncated Fourier series at the second order:

$$\lambda = -7.88 + 1.27\cos\left(\frac{day\cdot 2\pi}{365}\right) + 0.45\sin\left(\frac{day\cdot 2\pi}{365}\right) - \\ - 0.16\cos\left(2\frac{day\cdot 2\pi}{365}\right) - 0.73\sin\left(2\frac{day\cdot 2\pi}{365}\right) \quad (20)$$

where *day* corresponds to the Julian date (1 = 1 January, 365 = 31 December). We evaluated the accuracy of this approach comparing the model output values with daily data measured by the AWS1 Forni during 2010.

2.5. *Model validation*

We used a number of descriptive statistics to validate shortwave and longwave radiation, and air temperature. We calculated bias (*BE*) as:

$$BE = \frac{1}{N}\sum(y - x) \quad (21)$$

where *N* is sample size, and *y* and *x* are measured and modelled values, respectively. Secondly, we estimated the mean absolute error (*MAE*) as:

$$MAE = \frac{1}{N}\sum|y - x| \quad (22)$$

Third, the root mean square error (*RMSE*) was calculated as:

$$RMSE = \left[\frac{1}{N}\sum(y - x)^2\right]^{0.5} \quad (23)$$

Finally, we calculated bias-removed root mean square error (*BRRMSE*) as:

$$BRRMSE = \left[\frac{1}{N}\sum(y - x - BE)^2\right]^{0.5} \quad (24)$$

3. RESULTS AND DISCUSSIONS

Figure 7 shows the spatial distribution of the exo-atmospheric solar radiation over the Forni Glacier during the spring and autumn equinoxes, and summer and winter solstices, considering real surfaces and neglecting the effects of shading by surrounding topography and atmospheric absorption. As expected, the day with the highest solar radiation is the summer solstice (with 41.9 MJ m^{-2}). The largest cumulative annual value (about 12000 MJ m^{-2}) is reached on a south-facing surface with a slope of 22.7°, while the smallest one (about 1350 MJ m^{-2}) is observed on a north-facing surface with a slope of 62.8°. Auto-shading conditions (estimated according to Allen & *alii*, 2006) occur for northerly facing slopes higher than 23.3°. Particularly, whenever the slope exceeds 70° auto-shading can occur every day. Generally, the northern part of the eastern basin features the most intense solar irradiation on the glacier. Here the slopes are moderate and the main aspect is south and south-west (fig. 7). The $SW_{T\text{-}AWS}/SW_{0\text{-}AWS}$ ratio measured at AWS1 Forni ranges from 0.1 to 1.3. Taking into account both cloudiness and multi-reflection, this well agrees with the range 0.2-1.2 found by Hock (1999).

Validation of our approach was performed by comparing the modelled incoming shortwave radiation against the one measured at 18 sites along the glacier tongue, during summer 2011 and 2012 (fig. 8).

The model agrees well with observations (tab. 1), with an r value of 0.97.

The estimated values of daily mean LW_{in} were compared against those by the AWS1 Forni during 2006-2012 period (fig. 9). The model performance was evaluated during the actual glacier ablation period (i.e.: May-September in agreement with Oerlemans, 2000). In fact on the other months (i.e.: October-April) at the Forni Glacier accumulation prevails (Senese & *alii*, 2014), thus neglecting this latter period is acceptable since the main aim of our work is at modelling radiative components driving glacier melt. An acceptable agreement between the two datasets was found (tab. 1), although there was a significant share of points with LW_{in} underestimated by the model. This can be due to neglecting the local topography, but probably the most important factor is poor cloudiness computation. Indeed, a low modelled longwave radiation is likely due to the presence of clouds, increasing the column-averaged temperatures and thus down-welling longwave radiation. Another source of errors is probably linked to the fact that the temperature of the lowest air layers over the glacier may be affected by the temperature of the glacier surface, which can cause, especially in summer, temperature inversions above the glacier. Therefore, in warm conditions, temperatures measured at glacier AWS may underestimate longwave irradiance as they may be more representative of the

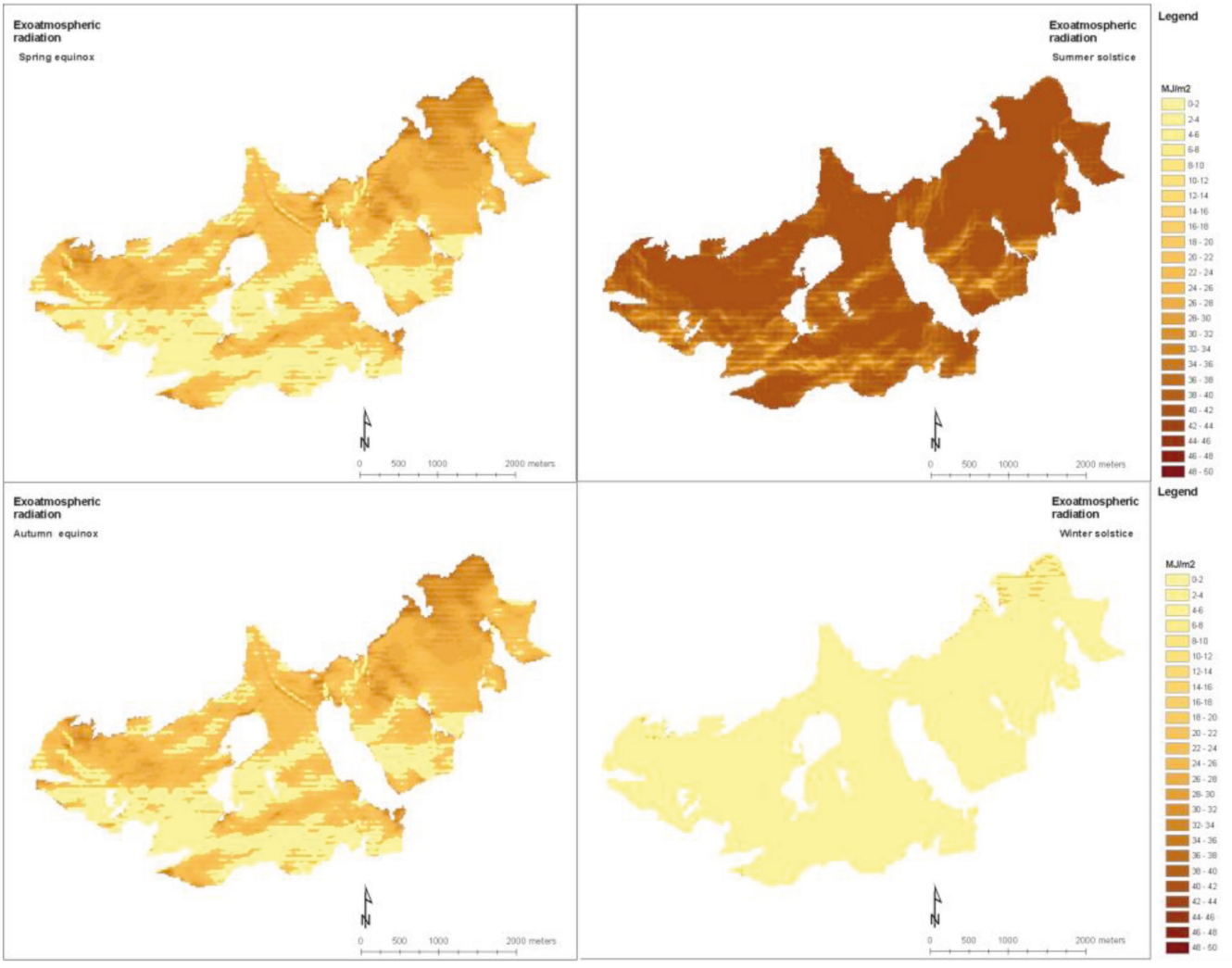

FIG. 7 - Maps of daily exo-atmospheric solar radiation over the Forni Glacier during the spring and autumn equinoxes and summer and winter solstices, considering real surfaces and neglecting the effects of shading by surround topography and atmospheric absorption.

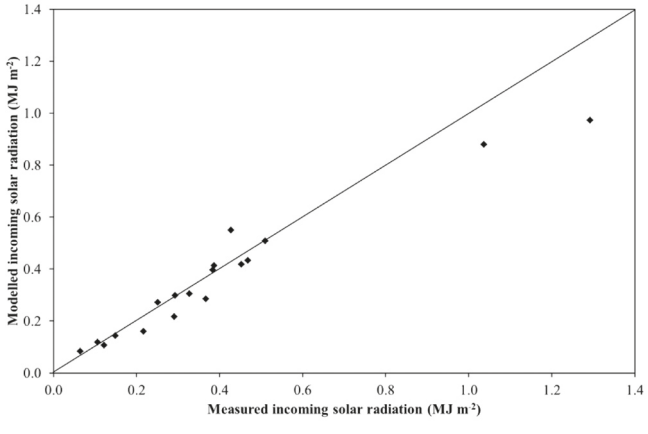

FIG. 8 - Measured and modelled incoming solar radiation during summer 2011 and 2012.

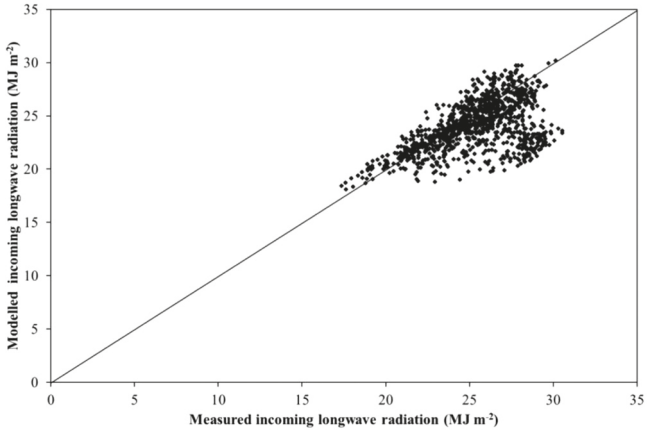

FIG. 9 - Modelled and measured daily incoming longwave radiation during May-September time frame from 2005 to 2012.

TABLE 1 - Statistical analyses about the applied methods for modelling shortwave and longwave radiation and air temperature

	BE	MAE	RMSE	BRRMSE
Shortwave radiation (MJ m^{-2})	*0.033*	*0.057*	*0.095*	*0.089*
Longwave radiation (MJ m^{-2})	*1.35*	*1.93*	*2.76*	*2.40*
Air temperature (°C)	*1.42*	*2.22*	*2.76*	*2.37*

melting surface than of the air over the glacier (van den Broeke, 1996). In our case, the underestimation is found to be consistent with cloudy sky conditions. Indeed, comparing daily differences measured-modelled LW_{in} (ΔLW_{in}) with cloudiness values (n), the 96.1% of ΔLW_{in} values higher than 5 MJ m^{-2} occurred with values of n higher than 0.8.

The approach presented in this paper can also be applied considering temperature as a function of elevation as described in Section 2.4, and applying some methodologies (see Shea & Moore, 2010) to extend the estimation of e_a over the entire glacier. We think, however, that the small vertical extent of the ablation area of the Forni Glacier (i.e.: from 2650 m a.s.l. to 3000 m a.s.l.) does not require such effort which instead has to be performed on widest mountain glaciers featuring a higher elevation extent.

Concerning air temperature, we shifted the daily air temperature values measured at Bormio (1225 m a.s.l.) to the AWS1 Forni site elevation (2631 m a.s.l.) applying the daily lapse rate (Eqn. 20). To validate this temperature reconstruction, we made a comparison between modelled daily air temperature values with air temperatures actually measured at the AWS1 Forni during 2010 (fig. 10). These two datasets result in agreement (tab. 1) with an r value of 0.95, but some points feature temperatures underestimated by the model. Nevertheless, the slope coefficient of the linear regression between measured and modelled temperatures is very close to 1 (fig. 10), thus suggesting that the approach is accurate enough. In a previous study (Senese & *alii*, 2014), we found that it was possible to perform a reasonable reconstruction of the supraglacial daily average air temperature at the AWS1 Forni starting from

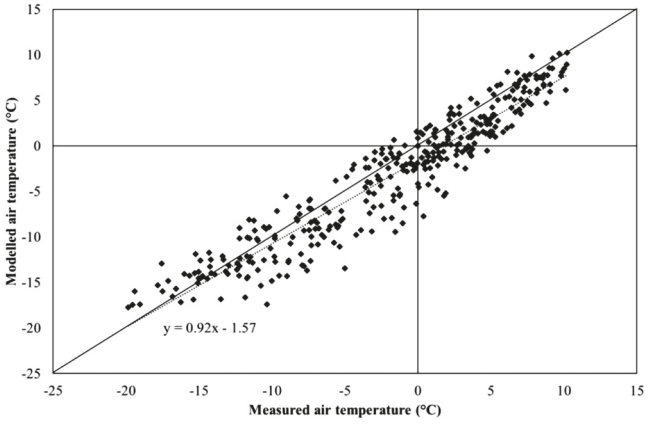

FIG. 10 - Modelled and measured daily air temperature during 2010 (the modeled series is derived from Bormio data shifted to the AWS1 Forni elevation through the application of estimated lapse rate, Eqn 20).

meteorological data acquired down valley using a mean tropospheric vertical gradient as lapse rate. Conversely, taking into account actual values of lapse rate (as the ones found in this study) allows a better distribution of air temperature over the whole surface of the glacier.

4. CONCLUSIONS

In the present study, we focus on modelling the meteorological parameters most influencing the snow/ice melting and on distributing them over a wide and representative alpine glacier, the Forni Glacier (Italian Alps, Stelvio National Park). In fact, in energy balance models the radiative components are the most important driving factors (Müller, 1985; Senese & *alii*, 2012a), while the air temperature is considered a proxy of ablation in T-index approaches (Braithwaite, 1995), thus requiring accurate reconstruction and distribution of data.

Firstly, the solar radiation was estimated taking into account astronomical and geographical factors and actual atmosphere conditions, secondly it was distributed considering slope and aspect of each glacier grid point, and shading due to the surrounding topography. The obtained solar radiation distribution was benchmarked against distributed solar radiation data measured during field campaigns in summer 2011 and 2012 (18 sites). The two datasets are in agreement with a RMSE of 0.095 MJ m^{-2}, thus suggesting that the proposed solar radiation model is suitable for the purpose. Then, we compared distributed measured longwave data (acquired by a portable net radiometer at several points at the glacier surface) to infrared values acquired simultaneously by the permanent supraglacial AWS installed at the surface of the Forni Glacier. The two records of data supported the assumption of spatially constant incoming longwave radiation may be taken as acceptable (as stated by Hock & Noetzli, 1997). Then we modelled daily infrared values from 2006 to 2012 (during May-September) and we compared the obtained data to the ones measured by the AWS1 Forni. It resulted only 12.3% of the samples featuring an underestimation larger than 5 MJ m^{-2}, and the underestimation not exceeding 8 MJ m^{-2} thus supporting our approach. A higher measured incoming longwave radiation with respect to the modelled one is probably due to the presence of clouds, increasing the column-averaged temperatures and thus down-welling longwave radiation, and to the surrounding topography. Hence, the infrared model can be considered appropriate and the observed underestimation possibly negligible. Finally, the air temperature was estimated considering long temperature records (2006-2009 dataset), different mea-

surement stations (Bormio, 1225 m a.s.l., Santa Caterina Valfurva, 1730 m a.s.l., and Frodolfo dam, 2180 m a.s.l.), and general meteorological conditions (such as excluding thermal inversion). Then, the modelled daily lapse rate was applied to Bormio dataset and the obtained values were validated against those from the AWS1 Forni during 2010. Even in this case, the model agrees well with observations (RMSE = 2.76°C). Eventually, the present study provided some information concerning errors in modelling solar and infrared radiation and air temperature, useful for quantifying glacier melt rate. Moreover, it turned out that unlike solar radiation and air temperature, the longwave radiation can be considered constant over a glacier surface. In conclusion, for estimating these three parameters, we suggest that a supraglacial weather station measuring all meteorological data is not strictly necessary. In fact, air temperature can be modelled from data acquired far away the site: Bormio is about 20 km from the glacier terminus. The parameters that should be measured directly over the glacier surface (or at least very close to it) seem to be: i) the vapour pressure, considered in this study for estimating the clear-sky emissivity in the infrared model, and ii) the shortwave radiation. Hence, it seems enough a minimal configuration for a supraglacial weather station, equipped with a pyranometer measuring the incoming global solar radiation, and a thermo-hygrometer, for modelling of the three most important parameters driving the ice/snow melting.

In the near future, there will be more and more detailed DEM based on UAV reliefs (Fugazza & *alii*, 2015), thus allowing a more correct distribution of meteorological parameters. In addition, the next step of our research will be to use the parameterization presented in this study coupled with spatially distributed albedo derived from remote sensing (e.g. Fugazza & *alii*, 2016) for a more accurate description of the absorbed solar radiation at each glacier pixels. This last point is particularly important as the net radiation is certainly greater in recent times as a result of the darkening phenomena (Diolaiuti & Smiraglia, 2010), namely the increasing deposition of black carbon and dust on glacier surface which reduces albedo and increases melting (Azzoni & *alii*, 2016).

REFERENCES

Allen R.G., Trezza R. & Tasumi M. (2006) - *Analytical integrated functions for daily solar radiation on slopes*. Agricultural and Forest Meteorology, 139, 55-73.

Arnold N.S., Willis I.C., Sharp M.J., Richards K.S. & Lawson W.J. (1996) - *A distributed surface energy-balance model for a small valley glacier. I. Development and testing for Haut Glacier d'Arolla, Valais, Switzerland*. Journal of Glaciology, 42, 77-89.

ARPA Lombardia: http://www2.arpalombardia.it/siti/arpalombardia/meteo/richiesta-dati-misurati/Pagine /RichiestaDatiMisurati.aspx.

Azzoni R.S., Senese A., Zerboni A., Maugeri M., Smiraglia C. & Diolaiuti G. (2016) - *A novel integrated method to describe dust and fine supraglacial debris and their effects on ice albedo: the case study of Forni Glacier, Italian Alps*. The Cryosphere, 10, 665-679. doi: 10.5194/tc-10-665-2016.

Bintanja R. & van den Broeke M.R. (1996) - *The influence of clouds on the radiation budget of ice and snow surfaces in Antarctica and Greenland in summer.* International Journal of Climatology, 16(11), 1281-1296.

Blöschl G., Kirnbauer B. & Gutknecht D. (1991) - *Distributed snowmelt simulations in an Alpine catchment. 1. Model evaluation on the basis of snow cover patterns*. Water Resources Research, 27, 3171-79.

Bocchiola D., Senese A., Mihalcea C., Mosconi B., D'agata C., Smiraglia C. & Diolaiuti G.A. (2015) *An ablation model for debris-covered ice: the case study of Venerocolo Glacier (Italian Alps)*. Geografia Fisica e Dinamica Quaternaria, 38 (2), 113-128.

Braithwaite R.J. (1995) - *Positive degree-day factors for ablation on the Greenland ice sheet studied by energy-balance modelling.* Journal of Glaciology, 41, 153-60.

Brun E., Martin E., Simon V., Gendre C. & Coleou C. (1989) - *An energy and mass model of snow cover suitable for operational avalanche forecasting.* Journal of Glaciology, 35, 333-342.

Citterio M., Diolaiuti G., Smiraglia C., Verza G. & Meraldi E. (2007) - *Initial results from the automatic weather station (AWS) on the ablation tongue of Forni Glacier (Upper Valtellina, Italy).* Geografia Fisica e Dinamica Quaternaria, 30, 141-151.

D'Agata C., Bocchiola D., Maragno D., Smiraglia C. & Diolaiuti G. (2014) - *Glacier shrinkage driven by climate change in The Ortles-Cevedale group (Stelvio National Park, Lombardy, Italian Alps) during half a century (1954-2007).* Theoretical and Applied Climatology, 116, 169-190.

Diolaiuti G. & Smiraglia C. (2010) - *Changing glaciers in a changing climate: how vanishing geomorphosites have been driving deep changes in mountain landscapes and environments*. Geomorphologie, 2, 131-152.

Duffie J.A. & Beckman W.A. (1980) - *Solar Engineering of Thermal Process*, 1st ed. John Wiley and Sons, New York.

Ellingston R.G., Ellis J. & Fels S. (1991) - *The intercomparison of radiation codes used in climate models: long-wave results*. Journal of Geophysical Research, 96, 8929-8953.

Escher-Vetter H. (1980) - *Der strahlungshaushalt des Vernagtferners als Basis der Energiehaushaltsberechnung zur bestimmung der Schmelzwasserproduktion eines Alpengletschers*. Vol. 39. Universität München.

Fugazza D., Senese A., Azzoni R.S., Smiraglia C., Cernuschi M., Severi D. & Diolaiuti G.A. (2015) - *High resolution mapping of glacier surface features. The UAV survey of the Forni Glacier (Stelvio National Park, Italy)*. Geografia Fisica e Dinamica Quaternaria, 38(1), 25-33.

Fugazza D., Senese A., Azzoni R.S., Maugeri M., Diolaiuti G.A. (2016) - *Spatial distribution of surface albedo at the Forni Glacier (Stelvio National Park, Central Italian Alps)*. Cold Regions Science and Technology 125, 128-137. http://dx.doi.org/10.1016/j.coldregions.2016.02.006

Gambelli S., Senese A., D'agata C., Smiraglia C. & Diolaiuti G. (2014) - *Preliminary analysis for distribution of the surface energy budget of the Forni Glacier, Valtellina (Ortles-Cevedale Group, Italy).* Geografia Fisica e Dinamica Quaternaria, 37(1), 15-22. DOI 10.4461/GFDQ.2014.37.2

Garner B.J. & Ohmura A. (1968) - *A method for calculating direct shortwave radiation income of slopes*. Journal of Applied Meteorology, 7, 796-800.

Granger R.J. & Gray D.M. (1990) - *A net radiation model for calculating daily snowmelt in open environments*. Nordic Hydrology, 21(4-5), 217-234.

GREUELL W., KNAP W.H. & SMEETS P.C. (1997) - *Elevational changes in meteorological variables along a midlatitude glacier during summer.* Journal of Geophysical Research: Atmospheres (1984-2012), 102(D22), 25941-25954.

GUEYMARD C. (1993) - *Critical analysis and performance assessment of clear-sky solar-irradiance models using theoretical and measured data*. Solar Energy, 51(2), 121-38.

GUEYMARD C.A. (2001) - *Parameterized transmittance model for direct beam and circumsolar spectral irradiance.* Solar Energy, 71 (5), 325-346.

HOCK R. (1999) - *A distributed temperature-index ice- and snowmelt model including potential direct solar radiation*. Journal of Glaciology, 45 (149), 101-111.

HOCK R. (2005) - *Glacier melt: a review of processes and their modelling.* Progress in Physical Geography, 29, 362.

HOCK R. & HOLMGREN B. (2005) - *A distributed surface energy-balance model for complex topography and its application to Storglaciaren, Sweden*. Journal of Glaciology, 51(172), 25-36.

HOCK R. & NOETZLI C. (1997) - *Areal melt and discharge modeling of Störglaciaren, Sweden*. Annals of Glaciology, 24, 997.

HUNTER G.J. & GOODCHILD M.F. (1997) - *Modeling the uncertainty of slope and aspect estimates derived from spatial databases*. Geographical Analysis, 29 (1), 35-49.

IQBAL M. (1983) - *An introduction to solar radiation*. Academic Press, Orlando, FL., OSTI ID: 5596615.

KLOK E.J. & OERLEMANS J. (2002) - *Model study of the spatial distribution of the energy and mass balance of Morteratschgletscher, Switzerland*. Journal of Glaciology, 48, 505-18.

KONDRATYEV K.Y. (1969) - *Radiation in the atmosphere*. New York: Academic Press, 912 pp.

KONZELMANN T., VAN DE WAL R.S., GREUELL W., BINTANJA R., HENNEKEN E.A. & ABE-OUCHI A. (1994) - *Parameterization of global and longwave incoming radiation for the Greenland Ice Sheet*. Global and Planetary change, 9(1), 143-164.

KONZELMANN T. & OHMURA A. (1995) - *Radiative fluxes and their impact on the energy balance of the Greenland ice sheet*. Journal of Glaciology, 41(139), 490-502.

MÜLLER H. (1985) - *On the radiation budget in the Alps.* International Journal of Climatology, 5(4), 445-462.

OERLEMANS J. (2000) - *Analysis of a 3 years meteorological record from the ablation zone of Morteratschgletscher, Switzerland: energy and mass balance*. Journal of Glaciology, 46 (155).

OERLEMANS J. (2001) - *Glaciers and Climate Change*, Lisse, Balkema.

OKE T.R. (1987) - *Boundary layer climates*. Second edition. London, Methuen, New York, Routledge Press. 435 pp.

PLÜSS C. & OHMURA A. (1997) - *Longwave radiation on snow-covered mountain surfaces*. Journal of applied meteorology, 36, 818-824.

SAUBERER F. (1955) - *Zur Abschätzung der Globalstrahlung in verschiedenen Höhenstufen der Ostalpen*. Wetter und Leben, 7, 22-29.

SEDLAR J. & HOCK R. (2009) - *Testing longwave radiation parameterizations under clear and overcast skies at Storglaciären, Sweden*. The Cryosphere, 3(1), 75-84.

SENESE A., DIOLAIUTI G., MIHALCEA C. & SMIRAGLIA C. (2012a) - *Energy and mass balance of Forni Glacier (Stelvio National Park, Italian Alps) from a 4-year meteorological data record*. Arctic, Antarctic, and Alpine Research, 44 (1), 122-134.

SENESE A., DIOLAIUTI G., VERZA G.P. & SMIRAGLIA C. (2012b) - *Surface energy budget and melt amount for the years 2009 and 2010 at the Forni Glacier (Italian Alps, Lombardy).* Geografia Fisica e Dinamica Quaternaria, 35 (1), 69-77.

SENESE A., MAUGERI M., VUILLERMOZ E., SMIRAGLIA C. & DIOLAIUTI G. (2014) - *Using daily air temperature thresholds to evaluate snow melting occurrence and amount on Alpine glaciers by T-index models: the case study of the Forni Glacier (Italy).* The Cryosphere, 8, 1921-1933. doi:10.5194/tc-8-1921-2014

SHEA M.J. & MOORE R.D. (2010) - *Prediction of spatially distributer regional-scale fields of air temperature and vapor pressure over mountain glaciers*. Journal of Geophysical research, 115, D23107

SICART J.E., POMEROY J.W., ESSERY R.L.H. & BEWLEY D. (2006) - *Incoming longwave radiation to melting snow: observations, sensitivity, and estimation in northern environments*. Hydrological Processes, 20(17), 3697-3708.

SPENCER J.W. (1971) - *Fourier series representation of the position of the sun*. Search, 2, 172 pp.

VAN DEN BROEKE M. (1996) - *Characteristics of the lower ablation zone of the west Greenland ice sheet for energy-balance modelling.* Annals of Glaciology 23, 160-66.

WANG Q., TENHUNEN J., SCHMIDT M., KOLCUN O. & DROESLER M. (2006) - *A model to estimate global radiation in complex terrain*. Boundary-Layer Meteorology, 119, 409-429.

(Ms presented 15 January 2015; accepted 15 April 2016)

Edizioni ETS
Piazza Carrara, 16-19, I-56126 Pisa
info@edizioniets.com - www.edizioniets.com
Finito di stampare nel mese di ottobre 2016